Various Power Management Schemes For Efficient Wind Energy Conversion System

Rupendra Pachauri, Ankur Kumar Gupta, Raj Gaurav Mishra, Yogesh Chauhan

Abstract: In this paper, various control schemes of power management based on wind turbine (blade pitch angle or/and tip speed ratio), load parameters (current, voltage, power) and permanent magnet synchronous generator (PMSG) parameter (rotor speed) are proposed with simple and easy to implement Proportional-Integral (PI) controller for wind energy conversion system (WECS) operation. These control systems can be used for the purpose of power management. Together with these control schemes, the proposed WECS model is implemented in the MATLAB / Simulink environment. The operation of a WECS system is tested under dynamic conditions with these proposed control schemes. The results show that performance of these schemes is found satisfactory and based on these results, a comparative study is done.

Index Terms: Power management schemes, wind turbine, renewable energy, blade pitch angle, tip speed ratio control, wind energy conversion system, performance coefficient.

1 Introduction

THE scarcity of the fossil fuels is increasing exponentially as well as consumption of energy. Due to this, there is an urgently require to recognize more sustainable sources of energy to meet energy demand. There is extensive exploration of renewable energy (RE) sources such as solar PV (Photovoltaic) system, wind and fuel cell etc. In this context, the wind energy is considered as one of the most promising alternative source of energy for power generation [1]. One of the most important issues in WECS is to harness maximum possible energy from the wind in minimum effort and time duration, which can be achieved through various power management methods [2]. Although, different types of wind turbines are available; Variable Speed Wind Turbine (VSWT) systems are one of the most suitable type of wind turbine for electric power generation. Generally, the VSWT-based WECS system consists of a dual fed induction generator (DFIG) and a permanent synchronous magnet generator (PMSG). Due to recent developments in power electronics devices and their improved reliability and efficiency, the utilization of PMSG based WECS is growing rapidly. Currently, various controlled parameters of WECS such as blade pitch angle, WT torque, tip speed ratio, duty cycle of converter etc. are controlled which can be observed from Table 1.

- *Dr. Rupendra Pachauri is currently working as an Assistant Professor (Sr. Scale) in the Department of Electrical and Electronics Engineering, School of Engineering, University of Petroleum and Energy Studies, Dehradun, India, PH-+91-7455077626. E-mail: rpachauri@ddn.upes.ac.in*
- *Mr. Ankur Kumar Gupta is currently working as an Assistant Professor in the Department of Electrical Engineering, Model Institute of Engineering and Technology, Kotbhalwal, Jammu, India, E-mail: ankurradikal@gmail.com*
- *Mr. R. G. Mishra is currently working as an Assistant Professor (Sel. Scale) in the Department of Electrical and Electronics Engineering, School of Engineering, University of Petroleum and Energy Studies, Dehradun, India, Email: rgmishra@ddn.upes.ac.in*
- *Dr. Yogesh K. Chauhan is currently working as an Associate Professor in the Department of EE, KNIT, Sultanpur, Uttar Pradesh, India, Email: chauhanyk@yahoo.com*

TABLE 1

TYPICAL WECS CONTROL SCHEMES AND PARAMETERS [3-32]

Authors'	Year	Controlled parameters	Technique/ Controller	Generator used	Ref.
Senjyu et al.	2006	β , τ	PI, FLC	IG	[3]
Jauch et al.	2007	β	PID	---	[4]
Boukhezzar et al.	2007	β , τ	PID	---	[5]
Tous et al.	2008	β	PI	---	[6]
Zhang et al.	2008	β	PI, FLC	---	[7]
No et al.	2009	β	PI	IG	[8]
Yilmaz et al.	2009	β	ANN	IG	[9]
Abbas et al.	2010	ω	PI	SEIG	[10]
Musyafa et al.	2010	β	FLC	---	[11]
Errami et al.	2010	β , τ	PI	PMSG	[12]
Ciobotaru et al.	2010	Duty cycle	Hybrid DC-DC converter	PMSG	[13]
Izumi et al.	2011	β	PI	PMSG	[14]
Izumi et al.	2011	β	FLC	PMSG	[15]
Joseph et al.	2012	Duty cycle	Hill climbing method	PMSG	[16]
Chowdhury et al.	2012	β	FLC	IG	[17]
Abdullah et al.	2012	β , λ , τ power	PI	PMSG	[18]
Belghazi et al.	2012	β	GA	---	[19]
Vidal et al.	2012	β , τ , yaw	PI	---	[20]
Hwas et al.	2012	β	PI	DFIG	[21]
Barambones et al.	2012	β	Sliding mode	IG	[22]
Tabrizi et al.	2013	β	PI	PMSG	[23]
Petkovic et al.	2013	C_p	ANFIS	---	[24]
Howlader et al.	2013	β	PI	PMSG	[25]
Guo et al.	2013	β	FLC, PID	--	[26]
Goyal et al.	2013	β	Adaptive fuzzy PID	IG	[27]
Echchaachouai et al.	2014	Duty cycle	FOC	PMSG	[28]
Nasiri et al.	2014	λ , τ	PI	PMSG	[29]
Ran et al.	2014	WT	PID	PMSG	[30]

		speed			
Viveiros et al.	2015	β	PI, FLC	DFIG	[31]
Vargas et al.	2015	β	PI	PMSG	[32]

Blade pitch angle (BPA) =β , Torque = τ , Tip speed ratio (TSR)= λ ,Rotor speed = ω , Performance coefficient=Cp.

Moreover, the present paper is to show a comparative analysis for power management schemes of WECS such as current, voltage, power, blade pitch angle, tip speed ratio and rotor speed with the motivation of the above literature evaluation. Broadly, these power management schemes are categorized into three types based on (i) WT parameter control (ii) load parameter control (iii) PMSG parameter control. Some of the control schemes of power management are not reported in the literatu[illegible] b[illegible] the [illegible]wledge.

2 SY[illegible]E[illegible]ION

The co[illegible] sy[illegible] d[illegible] into four major parts: (a) WECS [illegible] (b) Control schemes for power management as (i) WT parameters based control schemes (BPA and TSR based torque control schemes) (ii) Load parameters based control schemes (current, voltage and power control schemes) (iii) PMSG parameters based control schemes (speed control of PMSG based scheme) (c) Power electronics interface using DC-DC converter (d) Resistive load. The system u[illegible] is shown in Figure 1.

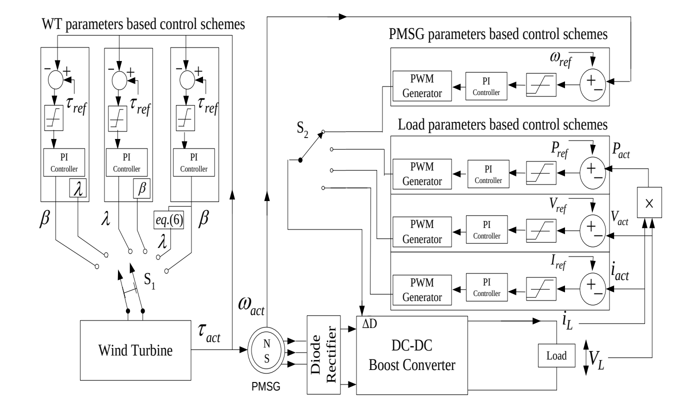

***Fig. 1.** WECS schematic diagram with suggested control schemes.*

Mechanical power of WT is calculated as,

$$P_m = \frac{1}{2}\rho A C_p(\lambda,\beta)V_w^3$$
(1)

Where, ρ is represenation for air density, A is expressed for WI swept area and V_w is wind speed. The power coefficient is represented by C_p which is non linear functions of tip speed ratio λ and blade pitch angle β as $C_p(\lambda,\beta)$ [33, 34]. The C_p has a theoretical value of 0.59 and expressed in Eq. (2) as,

$$C_p(\lambda,\beta) = c_1\left(\frac{c_2}{\lambda_i} - c_3\beta - c_4\right)e^{-\frac{c_5}{\lambda_i}} + c_6\lambda$$
(2)

Where,

$$\frac{1}{\lambda_i} = \frac{1}{\lambda + 0.08\beta} - \frac{0.035}{1+\beta^2}$$
(3)

The TSR λ is defined as,

$$\lambda = \frac{\Omega_t R}{V_w}$$
(4)

Where Ω_t is the speed rotor, R is expressed for the radius and V_w is stand for wind velocity. The developed mechanical torque τ_m of the wind turbine can be calculated as,

$$\tau_m = \frac{P_m}{\Omega_t}$$
(5)

The relation between C_P and λ is shown in Figure 2 (a)-(b) as,

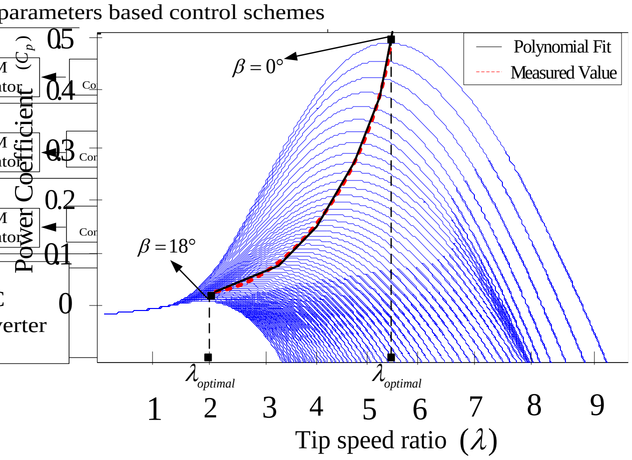

(a)

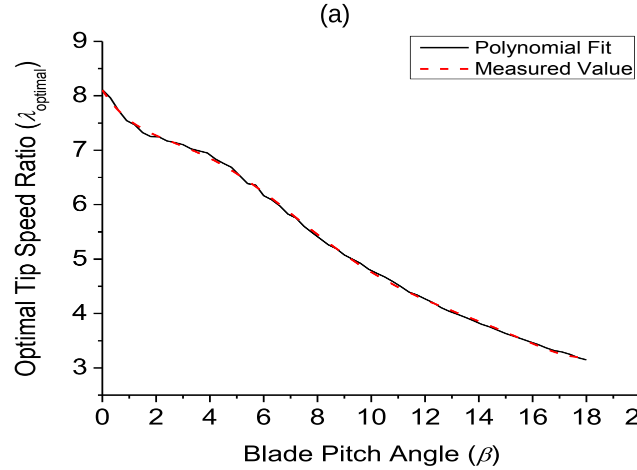

(b)

Fig. 2(a)-(b). Polynomial fit of measured data

From Figure 2(a) it is observed that the optimal value of the λ, varies with β for C_P to maximise. Therefore, a relation is expressed between both as β and $\lambda_{optimal}$ to improve C_P as shown in Eq. (6) as,

$$\lambda_{optimal} = \alpha - \gamma_1\beta + \gamma_2\beta^2 - \gamma_3\beta^3 + \gamma_4\beta^4 - \gamma_5\beta^5 + \gamma_6\beta^6$$
(6)

Eq. (6) is acquired by using polynomial fit method and plotted in Figure 2(b).

3.1 Modeling of permanent magnet synchronous generator (PMSG)

The PMSG model (mathematical) is established in the direct-quadrature (d-q) reference frame [35]. Which is in state equation and expressed by Eq. (7) and (8) as,

$$\frac{di_d}{dt} = \frac{1}{L_{ds} + L_{ls}}(-R_s i_d + \omega_e (L_{qs} + L_{ls}) i_q + u_d) \quad (7)$$

$$\frac{di_q}{dt} = \frac{1}{L_{qs} + L_{ls}}(-R_s i_q + \omega_e (L_{qs} + L_{ls}) i_d + u_q) \quad (8)$$

where, R_s is the stator resistance, i_d and i_q are the currents L_d and L_q are the generator induct. along the *d* and *q* axis and L_{ls} is the leakage induct. of the generator, and ω_e is the electrical rotating speed (rad/s) of the PMSG. The PMSG electromagnetic torque (EM) (T_{em}) is given by Eq. (9) as,

$$T_{em} = 1.5\,p((L_{ds} - L_{ls}) i_d i_q + i_q \psi_f) \quad (9)$$

where, ψ_f is the permanent magnetic flux.

4 MATLAB/SIMULINK MODEL OF WECS AND POWER MANAGEMENT SCHEMES

The model of WT has been implemented in MATLAB/Simulink and depicted in Figure 3. All the operating parameters used in the modeling of WT are listed in the Appendix.

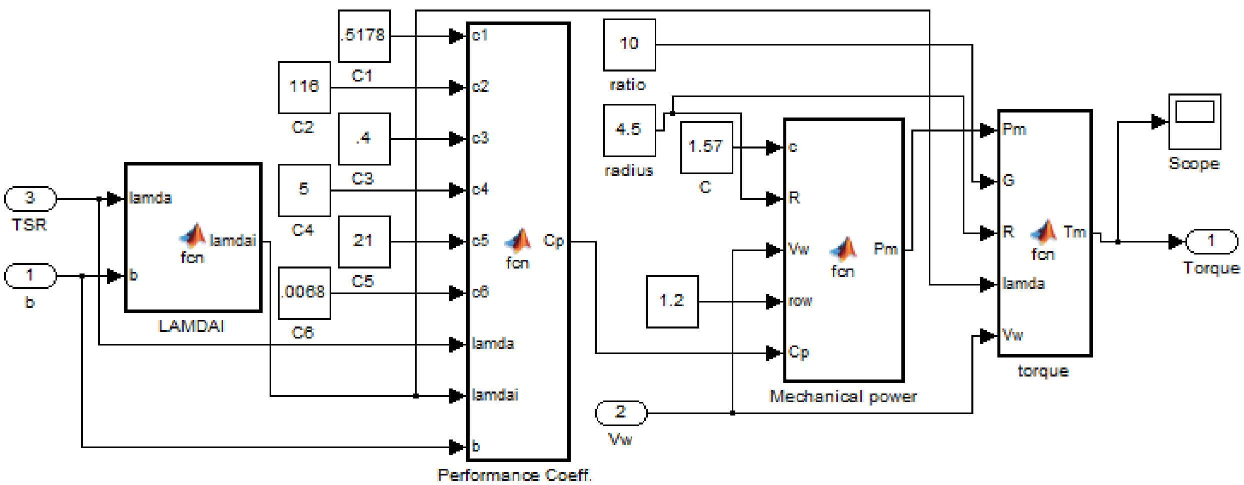

Fig. 3. MATLAB/Simulink model of WT

Different WECS power management control schemes depend on the signal processed in the control loop. This signal can be current, voltage, power, wind turbine parameters such as BPA, TSR and PMSG parameter such as rotor speed. The PI controller, which is easy to implement and efficient, is used for all these power control management schemes.

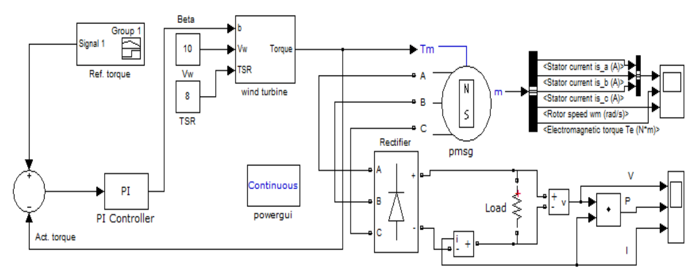

Fig. 4. MATLAB/Simulink model of BPA control scheme

4.1 WT parameter control schemes

4.1.1 Blade pitch angle control scheme

The MATLAB/Simulink model of BPA control scheme is depicted in Figure 4. BPA of WT is controlled using a PI controller. The error detector compares the reference and the actual torque. In addition, the PI controller processes this error signal, the output of which is the required BPA for WT.

4.1.2 TSR control scheme

Figure 5 shows the TSR-based power management control system MATLAB/Simulink model for WECS. WT's TSR is controlled by the PI controller. The error signal in torque is produced by comparing the actual and reference WT torque. The output signal i.e. TSR is produced by the PI controller and is proceed to the WECS.

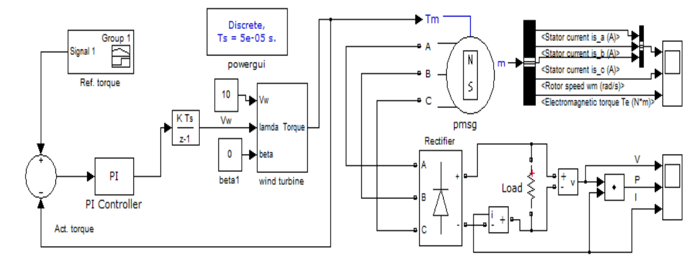

Fig. 5. *MATLAB/Simulink model of TSR control scheme*

4.1.3 BPA and TSR control scheme

The Simulink model of blade pitch angle and TSR control scheme affixed in Figure 6. In this model, by using Eq. (6) the TSR value is maintained at its optimum value accordingly with the actual BPA. This results in to the maximization of C_p. The error signal for the PI controller is generated by comparing the reference torque and actual WT torque. The outputs i.e. blade pitch angle and TSR of PI controller are fed to the WT for the power management of WECS.

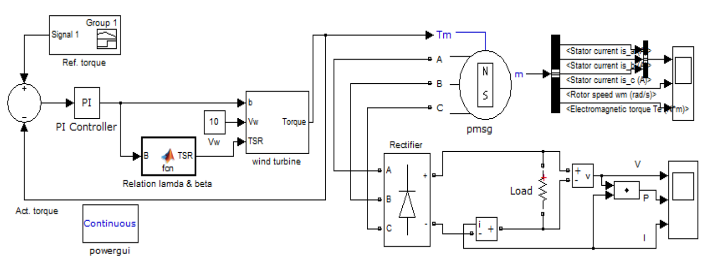

Fig. 6. *MATLAB/Simulink model of BPA and TSR control scheme*

4.2 Load parameters based control schemes

4.2.1 Current control scheme

The current control scheme Simulink model for WECS power management is shown in Figure 7. An error signal is generated by comparing the system's current reference and actual current, which is processed in the PI controller. In addition, the PI controller output is used to control the WECS DC-DC converter's duty ratio. For the entire load parameters based control schemes the β=0, λ =8 and V_w=10 m/sec are considered for WT.

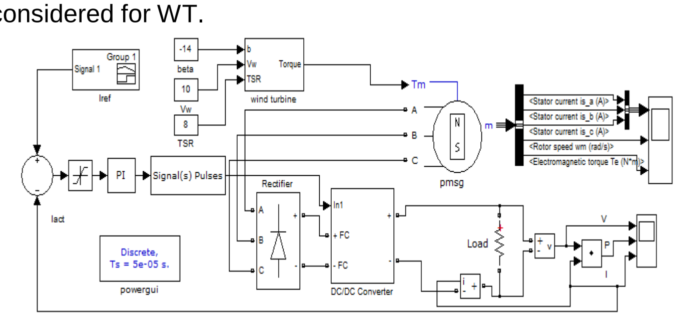

Fig. 7. *MATLAB/Simulink model of current control scheme*

4.2.2 Voltage control scheme

Figure 8 shows the MATLAB / Simulink voltage control scheme model. By evaluating and comparing the WECS reference voltage and actual voltage, the error signal is processed. This signal of error is used as the PI controller input. Furthermore, a pulse width modulation (PWM) generator is utilized to generate its output, which is the duty ratio of DC–DC converter.

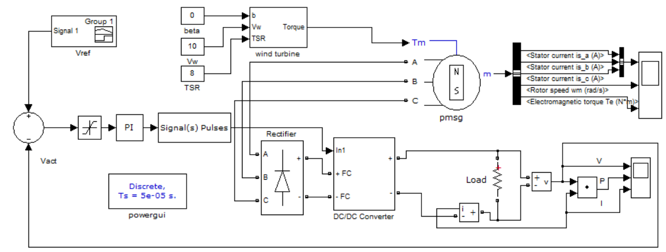

Fig. 8. *MATLAB/Simulink model of voltage control scheme*

4.2.3 Power control scheme

Figure 9 shows the WECS power control scheme model MATLAB/Simulink. Using the PI controller, the WECS reference and actual power are compared and evaluated. The output of PI controller, controls the width of pulse in the DC – DC converter generator producing the duty cycle.

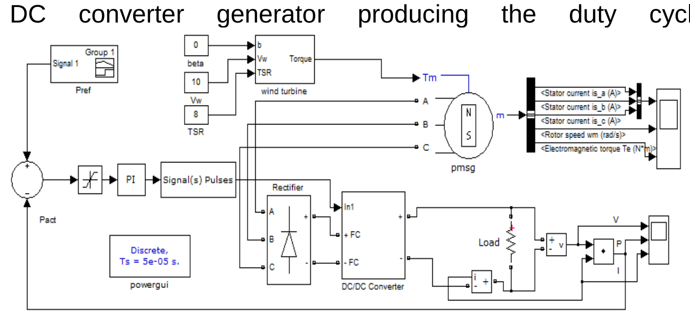

Fig. 9. *MATLAB/Simulink model of power control scheme*

4.3 PMSG parameters based control scheme

4.3.1 Rotor speed control scheme

The Simulink model of rotor speed control scheme (constant torque variable speed control) is shown in Figure 10. In this model reference and actual rotor speed of PMSG are compared and an error signal is obtained. This error signal is fed to the PI controller, which produces the duty ratio to control the output DC-DC converter.

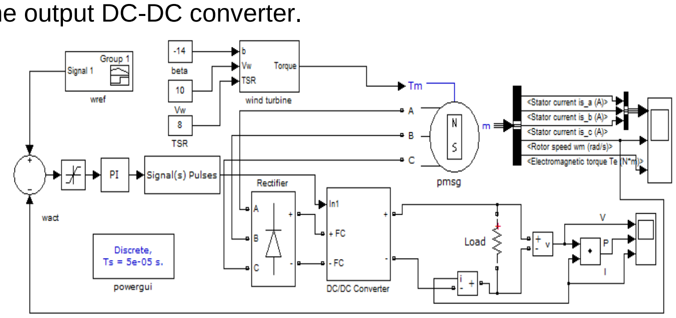

Fig. 10. *MATLAB/Simulink model of rotor speed control scheme*

5 Results and Discussion

Using developed simulation model, the performance parameters of the discussed power management schemes for WECS power management is analyzed and results are investigated for different dynamic conditions.

5.1 WT parameters control

5.1.1 Analysis of WECS with BPA control scheme

The transient performance of the BPA control scheme assisted WECS, is shown in Figure 11(a)-(e) in terms of reference torque (τ_{ref}), actual torque (τ_{act}), blade pitch angle (β), voltage (V) and current (I) respectively. The τ_{ref} is initially set at -12 Nm. The initial transient is settled within 0.53 sec and τ_{act} is gradually increasing to achieve the reference value. The system V and I are settled at 842.1V and 4.21A respectively, at this instant the value of β is 17.74^o. The τ_{ref} is step changed to -14 Nm at 2 sec. The τ_{act} follows the new τ_{ref} under the PI controller action and the system V and I are settle at 981.2V and 4.90A respectively within the transient duration of 0.22 sec. Now the β is decreased to 17.38^o for this value of $\tau_{ref.}$ Further, τ_{ref} changed to -18 Nm at 4 sec. The τ_{act} tracks the value of τ_{ref} and the system V and I settle at the values of 1258V and 6.289A respectively within the transient time 0.31 sec. Now the β is adjusted at 16.6^o. Furthermore, τ_{ref} is finally set at -14 Nm at 6 sec. The PI controller tracks the τ_{ref} by increasing the value of β. τ_{act} attains reference value of torque at 17.38^o (β) and the system V & I settle at the value of 981.2V & 4.9A respectively, within the transient period of 0.28 sec.

5.1.2 Analysis of WECS with TSR control scheme

The Simulink model of TSR control scheme employed for the power management of WECS system is shown in Fig. 12(a)-(e). The τ_{ref} is initially set at -12 Nm. With the PI controller action τ_{act} tracks the τ_{ref} and the initial dynamics are settled within 0.62 sec. The settled value of V & I are 841.6V & 4.20A respectively and the value of λ is settled at 12.33. The τ_{ref} is changed steply to -14 Nm at 2 sec. No significant transients are observed and system V & I are gradually increased to 981.1V and 4.91A respectively, now the value of λ is changed to 12.17. Further, τ_{ref} is set at -18 Nm at 4.0 sec. Due to this change, minute disturbance occurs in the system and the transient are settled within 0.57 sec. The value of settled λ is 11.86 and the corresponding system V & I are 1258V and 6.3A respectively. Further, τ_{ref} is finally set at -14 Nm at 6.0 sec. The τ_{act} tracks the reference value of torque using PI control action. The settled value of V & I are 981.2V & 4.9A respectively and corresponding value of λ is set at 12.17.

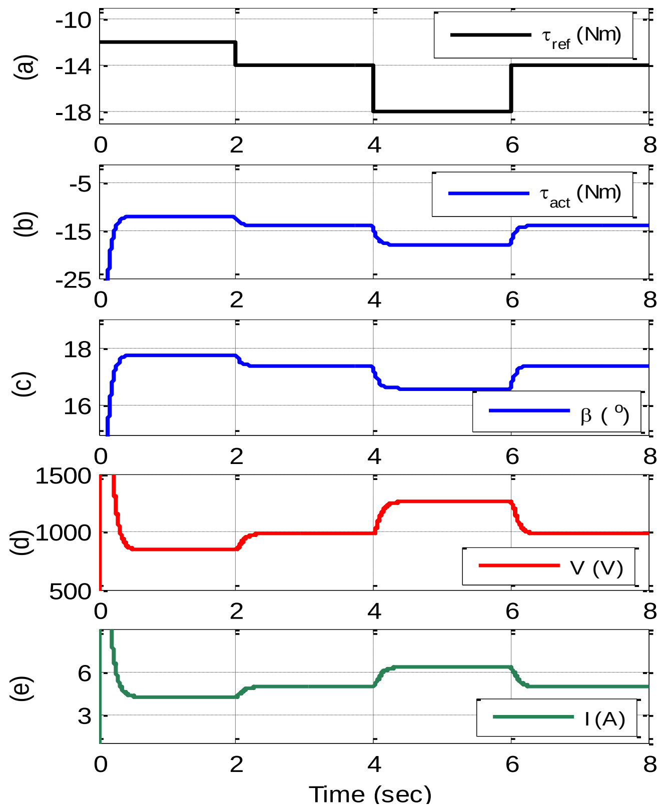

Fig. 11*(a)-(d). Performance of WECS with blade pitch angle control scheme*

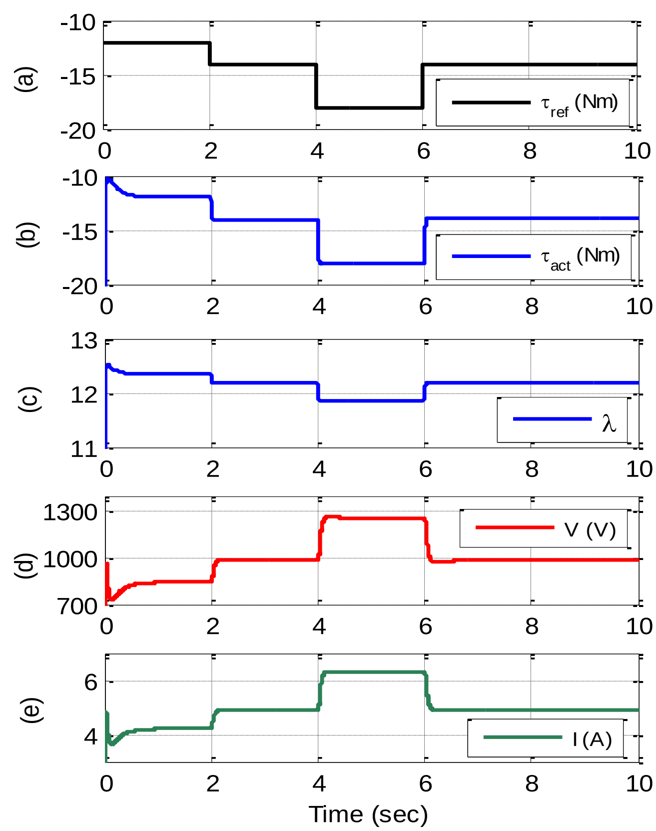

Fig. 12*(a)-(e). Performance of WECS with TSR control scheme*

5.1.3 Performance analysis of WECS with BPA and TSR control scheme

In this case, both β and λ of the WT parameters are controlled simultaneously, β is used as primary parameter to obtain the desired performance and λ is kept its optimal value corresponding to the actual value of β using Eq. (6). The dynamic performance of blade pitch angle and TSR control scheme, employed for power management of WECS is shown in Figure 13(a)-(f). The τ_{ref} is initially set at -12 Nm. The actual V & I are quickly settled at 842V & 4.2A within the period of 0.17 sec, at this instant the value of β and λ are 21.09^o and 6.7 respectively. Now the value of τ_{ref} is step reduced to -14 Nm at 2.0 sec, the parameters are gradually improved but speedily settled and τ_{act} is quickly raised to reference value of -14 Nm under the PI controller action. The system V & I are settled at 981.2V & 4.9A respectively and the value of λ and β at this instant are 6.62 and 21.03^o respectively. Further τ_{ref} is again step changed to -18 Nm. Due to this change, transients are occurred in system parameters which are quickly settled and the settled value of V & I are 1258V & 6.29A respectively. Now, the value of β and λ are decreased to 20.92^o and 6.35 respectively for this value of τ_{ref}. Moreover, the value of τ_{ref} is step increased and finally set at -14 Nm at 6 sec. The PI controller quickly tracks the reference value within the time period 0.05 sec and the settled value of V & I are 981.2V & 4.9A respectively. Here, the value of β and λ are set using the PI controller action at 21.03^o and 6.62 very shortly. The change in β and λ is quite measured which shows the effectiveness of used PI controller.

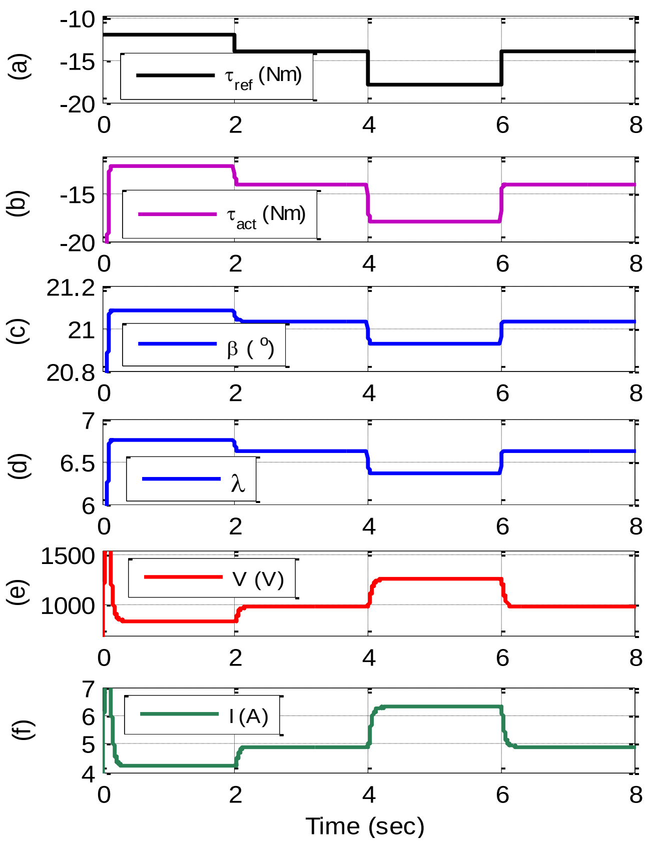

***Fig. 13**(a)-(d). Performance of WECS with BPA and TSR control scheme*

5.2 Load parameters based control schemes

5.2.1 Analysis of WECS with current control scheme

Figure 14(a)-(d) shows the dynamic performance of the current control scheme, which can be utilized for the power management of WECS in term of reference current (I_{ref}), actual current (I_{act}), voltage (V) and power (P). I_{ref} is varied in the range (2-4) A. Initially the I_{ref} is set at 2A. The initial transient are settled within 0.1 sec, during this time the transient are visible due to the initialization of PI controller and error is at maximum value during this time. Now the I_{ref} is step increased to 4A at 2 sec. As a result of this change, I_{act} tracks the I_{ref}; and V and P are settled at 812V and 3306W respectively within 0.16 sec. Furthermore, I_{ref} is decreased to 3A at 4 sec. The I_{act} tries to track this change. Because of this which, change in V and P occurs for around 0.45 sec and settled at 600V and 1864W respectively. Finally, the I_{ref} is set at 2.5A at 6.0 sec. Due to this change the V and P changes for 0.27 sec and then finally settled at 505.4V, 1252W respectively.

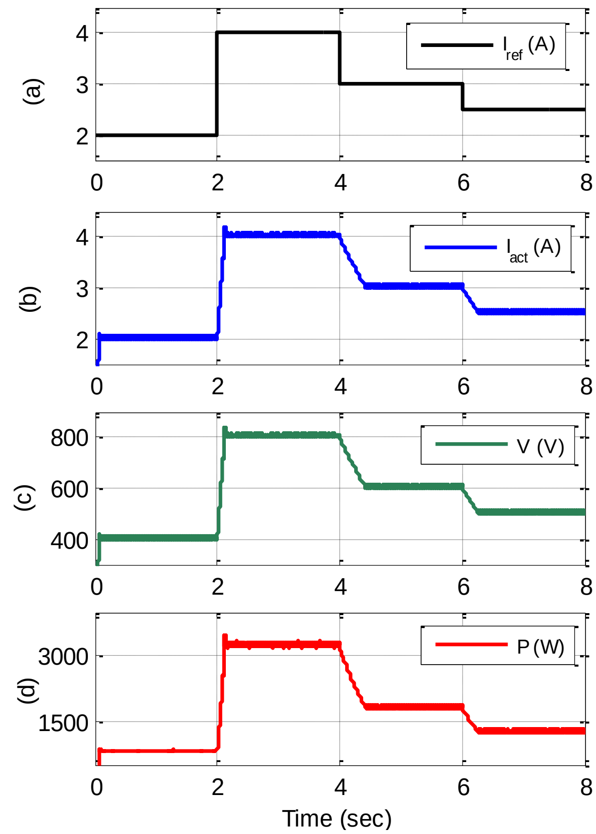

***Fig. 14**(a)-(d). Performance of WECS with current control scheme*

5.2.2 Performance analysis of WECS with voltage control scheme

The dynamic performance of voltage control scheme for WECS is shown in Figure 15(a)-(d) using reference voltage (V_{ref}), actual voltage (V_{act}), current (I) and power (P) respectively. In this case, the initial value of V_{ref} is set at 300V at t=0. After a short transient period of 0.12 sec, the V_{act} tracks V_{ref} and I & P are settled at 1.54A & 472W respectively. Now the V_{ref} is step increased to 400V at 2 sec. The change in V_{ref}, an increment in I and P are 2.04A, 835.5W respectively and the duration of transient period is insignificant. Further, the value of V_{ref} is increased to 500V at 4 sec. The V_{act} tries to track this change. Due to the effective of PI controller transient's period is only of 0.072 sec and the system *I* & *P* are settled at 2.539A and 1290W respectively. Furthermore, the V_{ref} is stepped increased to 350V. This large change in V_{ref} is tracked after a derivation of 0.53 sec due to effectiveness of PI control. The V_{act} tracks V_{ref} and system *I* & *P* are settled at 1.785A and 634.2W respectively.

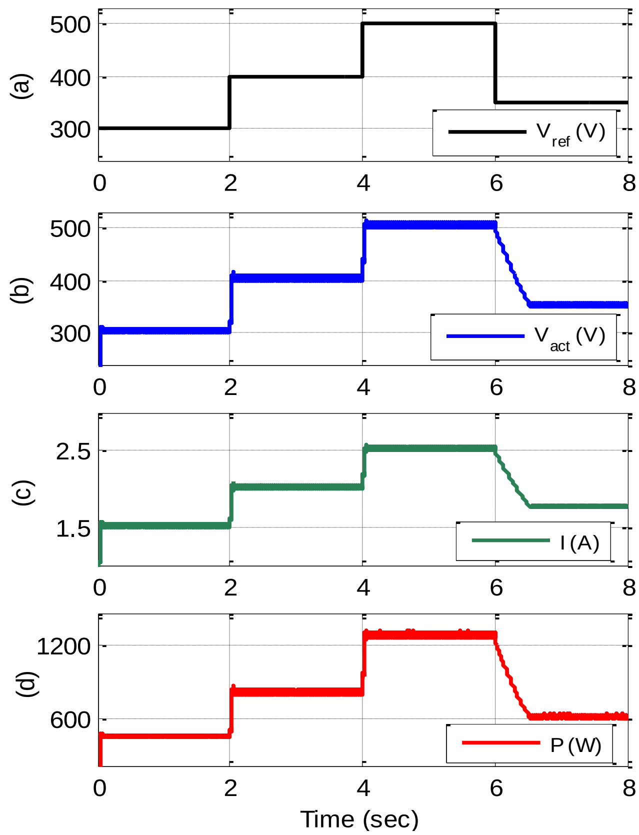

Fig. 15*(a)-(d). Performance of WECS with voltage control scheme*

5.2.3 Performance investigation of WECS with power control scheme

Figure 16(a)-(d) displays the transient analysis of the power scheme employed for WECS system. The P_{ref} is initially set at 1000W. After a short transient period of 0.252 sec, P_{act} is settled at reference value of 1000W after attaining a transient voltage of 450V. As well as, the WECS *V* & *I* are settled at 449.7V and 2.249A respectively. At 2 sec, the P_{ref} is suddenly increased to 1250W, as a result of this change, an increment in voltage and current of 502V and 2.502A is noticed respectively with transients duration of 0.12 sec. Now the P_{ref} is suddenly decreased to 1150W at 4 sec. Due to this change, the system *V* and *I* are settled at a steady state value of 502V and 2.508A respectively after a transient period of 0.1 sec. Furthermore, P_{ref} is finally decreased to 1050W, the P_{act} tries to follow this changed. The *V* and *I* are finally settled at 460V and 2.301A respectively at steady state.

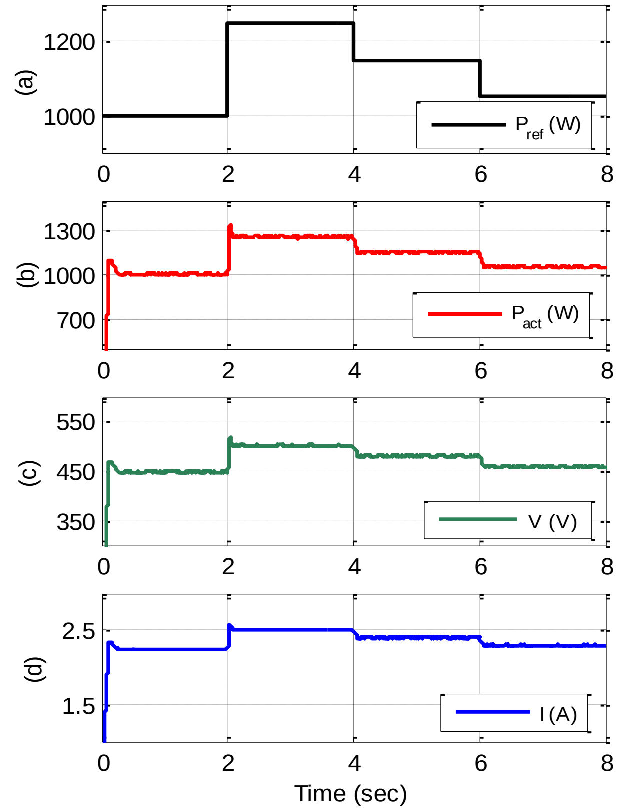

Fig. 16*(a)-(d). Performance of WECS with power control scheme*

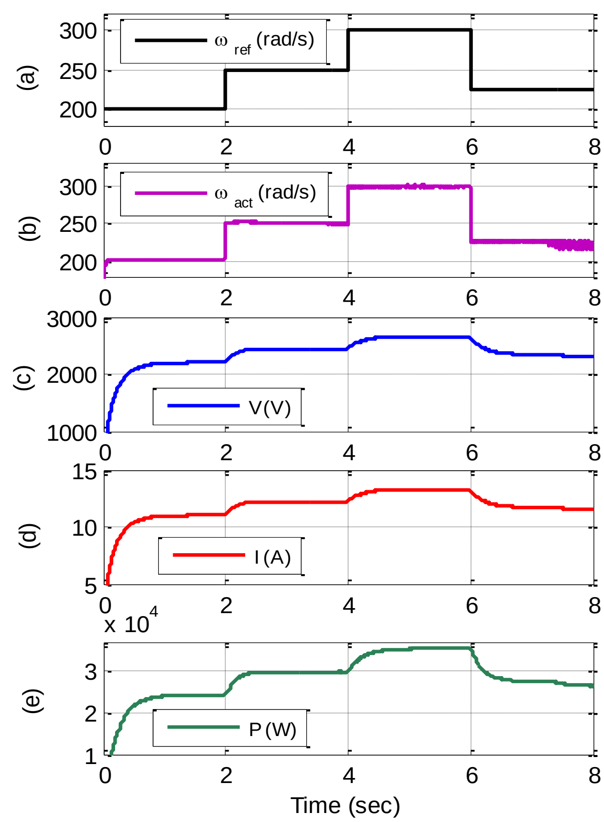

Fig. 17*(a)-(e). Performance of WECS with rotor speed control scheme*

5.3 PMSG parameters based control scheme

5.3.1 Performance analysis of WECS with rotor speed control scheme

In this case, the rotor speed (ω) of the PMSG is considered as a controlled parameter to obtain the desire performance from WECS. Figure 17(a)-(e) shows the dynamic performance of ω control scheme, employed for WECS. Initially, the ω_{ref} is set at 200 rad/sec. The tracking speed of the used controller in this case is slow as compared with the controllers used in other control schemes. The electrical transients are settled within the time period of 1.37 sec and the settled value of *V, I* & *P* are 2193V, 10.99A & 24180W respectively. Now, ω_{ref} is step increased to 250 rad/sec at 2.0 sec. Due to this change in ω_{ref} , gradual change is caused in system parameters; which is settled within the time duration of 0.438 sec. The system *V, I* & *P* are settled at 2432V, 12.15A & 29520W respectively. Further, the value of ω_{ref} is again step increase to 300 rad/sec at 4.0 sec. The PMSG ω_{act} tracks the ω_{ref} using PI controller and the transients are resolved within the time interval of 0.562 sec. The settled value of system *V, I* and *P* are 2657V, 13.28A and 35360W respectively. Moreover, the ω_{ref} is step decreased and finally set at 225 rad/sec at 6.0 sec. As a results of this change in ω_{ref} , the ω_{act} tries to attain the reference value using the PI controller action. The system *V, I* and *P* are settled at 2339V, 11.71A and 26590W respectively within the time interval of 1.27 sec. In this case, the PI controller action is quite observable to track the change in ω_{ref}. The major parameters of the dynamic analysis of the considered power management control schemes for WECS are summarized in Table 2. From Table 2, it can be concluded that the considered power management control schemes have satisfactory performance and are suitable for control of WT based power generation system. Furthermore, it can be observed that the performance of 'β - λ control scheme' is batter in terms settling time and transient response than other schemes.

TABLE 2

PERFORMANCE ANALYSIS OF POWER MANAGEMENT CONTROL SCHEMES

Type of control schemes	Name of control schemes	Settling Time (sec)				Transients at 5 sec.	
		at 0 sec	at 2 sec	at 4 sec	at 6 sec	Voltage (V)	Current (A)
WT parameters based control schemes	β control scheme	0.534	0.220	0.344	0.279	1258	6.288-6.289
	λ control scheme	0.615	0.190	0.460	0.328	1258	6.288-6.289
	β - λ control scheme	0.170	0.040	0.050	0.050	1258	6.289
Load parameters based control schemes	Current control scheme	0.100	0.160	0.450	0.270	600-630	3.0-3.05
	Voltage control scheme	0.120	0.080	0.072	0.537	500-510	2.50-2.55
	Power control scheme	0.252	0.123	0.095	0.125	479-482.10	2.395-2.410
PMSG parameter based control scheme	ω control scheme	1.371	0.438	0.562	1.270	2648-2655	13.25-13.28

6. CONCLUSION

This paper presented the analysis of the WECS system with distinguished proposed power management schemes. All the discussed control schemes are simulated in the MATLAB/Simulink GUI environment and under different loading conditions the analysis of discussed/proposed power management schemes is carried out. The main points of this study are,

- A number of new control schemes have been proposed for WECS, namely WT parameters (BPA or/and TSR), load parameters (load voltage, current and power), PMSG parameter (rotor speed) based control schemes.
- Based on mathematical model, The MATLAB/Simulink model is developed and validated through extensive results under dynamic conditions.
- In general, control schemes based on WT parameters are observed to have less transients than other techniques.
- Rotor speed based control scheme is observed to have slow tracking response.
- The overall performance of the WECS system was found satisfactory with these proposed new control schemes.

APPENDIX

WT parameters	
Number of blades	3
Blade radius (*R*)	4.5
Gear ratio (*G*)	40
Air density (ρ)	1.2 kg/m^3
Wind speed (V_W)	10-18 m/sec

Value of K_p and K_i for various control schemes	
K_p, K_i (Current control scheme)	500, 0.8
K_p, K_i (Voltage control scheme)	0.95, 0.30
K_p, K_i (Power control scheme)	0.94 0.35
K_p, K_i (β control scheme)	0.01, 3
K_p, K_i (λ control scheme)	0.01, 0.05

Power Coefficient (C_P)	0-0.59	K_p, K_i (β - λ control scheme)	0.01, 3
Tip speed ratio (λ)	7-9	K_p, K_i (ω control scheme)	1.9, 0.3
Blade Pitch angle (β)	0^o-18^o	**PMSG operating parameters**	
C_1 C_2	0.5176, 116	Stator Phase Resistance (R_s)	0.4250 ohm
C_3, C_4	0.4, 5	Inductance (L_d, L_q)	0.0084, 0.0084 H
C_5, C_6	21, 0.0068	Inertia (J_g)	0.001469 Kg m^2
α	8.105	Friction factor (F)	0.0003035 N m s
γ_1, γ_2	0.77, 0.28	No. of pole	2
γ_3, γ_4	0.061, 0.0059	Rated torque (τ_g)	-15 Nm
γ_5, γ_6	0.00027, 0.00000466	Rated voltage & current	1140V, 7.15 A

REFERENCES

[1] M A. Balat, "Review of Modern Wind Turbine Technology," Energy Sources, Part A: Recovery, Utilization, and Environmental Effects, vol. 14, pp. 1561-1572, 2009.

[2] Y. Errami, M. Ouassaid and M. Maaroufi, "Control of a PMSG Based Wind Energy Generation System for Power Maximization and Grid Fault Conditions," Energy Procedia, vol. 42, pp. 220-229, 2013.

[3] T. Senjyu, R. Sakamoto, N. Urasaki, T. Funabashi, H. Fujita and H. Sekine, "Output Power Leveling of Wind Turbine Generator for all Operating Regions by Pitch Angle Control", IEEE Transactions on Energy Conversion, vol. 21, pp. 467-475, 2006.

[4] C. Jauch, S. M. Islam, P. Sorensen and B. B. Jensen, "Design of a Wind Turbine Pitch Angle Controller for Power System Stabilization", Renewable Energy, vol. 32, pp. 2334-2349, 2007.

[5] B. Boukhezzar, L. Lupu, H. Siguerdidjane and M. Hand, "Multivariable Control Strategy for Variable Speed Variable Pitch Wind Turbines", Renewable Energy, vol. 32, pp.1273-1287, 2007.

[6] Y. E. Tous, "Pitch Angle Control of Variable Speed Wind Turbine", American Journal of Engineering and Applied Sciences, vol. 1, pp.118-120, 2008.

[7] J. Zhang, M. Cheng, Z. Chen and X. Fu, "Pitch Angle Control for Variable Speed Wind Turbines", Proc. IEEE Conference on Deregulation and Restructuring and Power Technologies, pp. 2691-2696, 2008.

[8] T. S. No, J. E. Kim, J. H. Moon and S. J. Kim, "Modeling, Control, and Simulation of Dual Rotor Wind Turbine Generator System", Renewable Energy, vol. 34, pp. 2124-2132, 2009.

[9] A. S. Yilmaz and Z. Ozer, "Pitch Angle Control in Wind Turbines above the Rated Wind Speed by Multi-Layer Perceptron and Radial Basis Function Neural Networks", Experts system with Applications. Vol. 36, pp. 9767-9775, 2009.

[10] F. A. R. Abbas and M. A. Abdulsada, "Simulation of Wind-turbine Speed Control by MATLAB", International Journal of Computer and Electrical Engineering, vol. 2, pp. 912-915, 2010.

[11] A. Musyafa, A. Harika, I. M. Y. Negara and I. Robandi, "Pitch Angle Control of Variable Low Rated Speed Wind Turbine Using Fuzzy Logic Controller", International Journal of Engineering and Technology, vol. 10, pp. 22-25, 2010.

[12] Y. Errami, M. Maaroufi and M. Ouassaid, "Modelling and Control Strategy of PMSG Based Variable Speed Wind Energy Conversion System", Proc. IEEE Conference on Multimedia Computing and Systems, pp. 1-6, 2010.

[13] C. K. Ciobotaru, R. Boraci, I. Filip, C. Vasar and G. Prostean, "Control Strategy for a Variable-Speed Wind Turbine Using DC Bus Measurements", Proc. IEEE Symposium on Intelligent Systems and Informatics, pp. 329-334, 2010.

[14] Y. Izumi, A. Pratap, K. Uchida, A. Uehara, T. Senjyu and A. Yona, "A Control Method for Maximum Power Point Tracking of a PMSG-based WECS Using Online Parameter Identification of Wind Turbine", Proc. IEEE Conference on Power Electronics and Drive Systems, pp. 1125-1130, 2011.

[15] Y. Izumi, A. Pratap, K. Uchida, A. Uehara, T. Senjyu and A. Yona, "A Fuzzy-Based Output Power Smoothing of WECS using Short-Term Ahead Prediction of Wind Speed", Proc. IEEE International Conference on Fuzzy Systems pp. 2414-2419, 2011.

[16] G. Joseph, J. C. Foreman and M. L. McIntyre, "A Variable Duty Cycle Maximum Power Point Tracking Algorithm for Wind Energy Conversion Systems", Proc. IEEE Conference on Power Electronics and Machines in Wind Applications, pp. 1-5, 2012.

[17] M. A. Chowdhury, N. Hosseinzadeh and W. X. Shen, "Smoothing Wind Power Fluctuations by Fuzzy Logic Pitch Angle Controller", Renewable Energy, vol. 38, pp. 224-233, 2012.

[18] M. A. Abdullah, A. H. M. Yatim, C. W. Tan and R. Saidur, "A Review of Maximum Power Point Tracking Algorithms for Wind Energy Systems", Renewable and Sustainable Energy Reviews, vol. 16, pp. 3220-3277, 2012.

[19] O. Belghazi and M. Cherkaoui, "Pitch Angle Control for Variable Speed Wind Turbines Using Genetic Algorithm Controller", Journal of Theoretical and Applied Information Technology, vol. 39, pp. 6-10, 2012.

[20] Y. Vidal, L. Acho, N. Luo, M. Zapateiro and F. Pozo, "Power Control Design for Variable Speed Wind Turbines", Energies, vol. 5, pp. 3033-3050, 2012.

[21] A. Hwas and R. Katebi, "Wind Turbine Control Using PI Pitch Angle Controller", Proc. IFAC Conference on Advances in PID Control, pp. 1-6, 2012.

[22] O. Barambones, J. M. G. D. Durana and M. D. L. Sen, "Robust Speed Control for a Variable Speed Wind Turbine", International Journal of Innovative Computing, Information and Control, vol. 8, pp. 7627-7640, 2012.

[23] H. Ye, J. Su, S. Du, "Simulation and Analysis of PMSG-based Wind Energy Conversion System Using Different Converter Models", Engineering Vol. 5, pp. 96-100, 2013.

[24] D. Petkovic, Z. Cojbasic and V. Nikolic, "Adaptive Neuro-Fuzzy Approach for Wind Turbine Power Coefficient Estimation", Renewable and Sustainable Energy Reviews, vol. 28, pp.191-195, 2013.
[25] A. M. Howlader, N. Urasaki and A. Yona, "A Review of Output Power Smoothing Methods for Wind Energy Conversion Systems", Renewable and Sustainable Energy Reviews, vol. 26, pp. 135-146, 2013.
[26] R. Guo, J. Du, J. Wu and Y. Liu, "The Pitch Control Algorithm of Wind Turbine Based on Fuzzy Control and PID Control", Energy and Power Engineering, vol. 5, pp. 6-10, 2013.
[27] S. Goyal, M. Gaur and S. Bhandari, "Power Regulation of a Wind Turbine Using Adaptive Fuzzy- PID Pitch Angle Controller", International Journal of Recent Technology and Engineering, vol. 2, pp. 128-132, 2013.
[28] A. Echchaachouai, S. E. Hani, A. Hammouch and S. Guedira, "A New Sensor Less Maximum Power Point Tracking Technologies of Wind Conversion Chain Based on a PMSG", Proc. IEEE Conf. on Renewable and Sustainable Energy, pp. 328-333, 2014.
[29] M. Nasiri, J. Milimonfared and S. H. Fathi, "Modeling, Analysis and Comparison of TSR and OTC Methods for MPPT and Power Smoothing in Permanent Magnet Synchronous Generator-based Wind Turbines", Energy Conversion and Management, vol. 86, pp. 892-900, 2014.
[30] C. Ran, J. Aiqiang, J. Jiapei, L. Ling and C. Tiantian, "An Improved Method of Maximum Peak Power Tracking Strategy for Wind Power Convention System", Proc. International Conference on Electricity Distribution, pp. 160-164, 2014..
[31] C. Viveiros, R. Melicio, J. M. Igreja and V. M. F. Mendes, "Supervisory Control of a Variable Speed Wind Turbine with Doubly Fed Induction Generator", Energy Experts, vol. 1, pp. 89-95, 2015.
[32] M. J. M. Vargas, D. G. O. Lorente, O. Rabaza and E. A. Hernandez, "Aggregated Models of Permanent Magnet Synchronous Generators Wind Farms", Renewable Energy, vol. 83, pp. 1-12, 2015.
[33] R. K. Pachauri and Y. K. Chauhan, "Mechanical Control Methods in Wind Turbine Operations for Power Generation", Journal of Automation and Control Engineering, vol. 2, pp. 214-220, 2012.
[34] J. Verma, Y. Tiwari, A. Mishra and N. Singh, "Performance, Analysis and Simulation of Wind Energy Conversion System Connected with Grid", International Journal of Recent Technology and Engineering, vol. 2, pp. 33-38, 2014.
[35] S. Li, T. A. Haskew, R. P. Swatloski and W. Gathings, "Optimal and Direct Current Vector Control of Direct-driven PMSG Wind Turbines", IEEE Transactions on Power Electronics, vol. 27, pp. 2325-2337, 2012.